

SIGHT: SINGLE-IMAGE CONDITIONED GENERATION OF HAND TRAJECTORIES FOR 3D HAND-OBJECT INTERACTION

Alexey Gavryushin¹✉ **Florian Redhardt**¹ **Gaia Di Lorenzo**¹ **Luc Van Gool**^{2,3}
Marc Pollefeys^{1,4} **Kaichun Mo**⁵ **Xi Wang**¹

¹ETH Zürich, Rämistrasse 101, 8092 Zürich, Switzerland

²KU Leuven, Oude Markt 13, 3000 Leuven, Belgium

³INSAIT, Sofia University, 15 Tsar Osvoboditel Blvd., 1504 Sofia, Bulgaria

⁴Microsoft Research, Seestrasse 356, 8038 Zürich, Switzerland

⁵NVIDIA, 4545 Roosevelt Way NE 6th Floor, Seattle, WA 98105, USA

ABSTRACT

We introduce a novel task of generating realistic and diverse 3D hand trajectories given a single image of an object, which could be involved in a hand-object interaction scene or pictured by itself. When humans grasp an object, appropriate trajectories naturally form in our minds to use it for specific tasks. Hand-object interaction trajectory priors can greatly benefit applications in robotics, embodied AI, augmented reality and related fields. However, synthesizing realistic and appropriate hand trajectories given a single object or hand-object interaction image is a highly ambiguous task, requiring to correctly identify the object of interest and possibly even the correct interaction among many possible alternatives. To tackle this challenging problem, we propose the SIGHT-Fusion system, consisting of a curated pipeline for extracting visual features of hand-object interaction details from egocentric videos involving object manipulation, and a diffusion-based conditional motion generation model processing the extracted features. We train our method given video data with corresponding hand trajectory annotations, without supervision in the form of action labels. For the evaluation, we establish benchmarks utilizing the first-person FPHAB and HOI4D datasets, testing our method against various baselines and using multiple metrics. We also introduce task simulators for executing the generated hand trajectories and reporting task success rates as an additional metric. Experiments show that our method generates more appropriate and realistic hand trajectories than baselines and presents promising generalization capability on unseen objects. The accuracy of the generated hand trajectories is confirmed in a physics simulation setting, showcasing the authenticity of the created sequences and their applicability in downstream uses.

1 INTRODUCTION

As our hand grasps an object, we immediately plan out potential maneuvers to manipulate it for our intentions. Consider pouring some juice from a bottle into a cup – it can be as straightforward as rotating your wrist. At a granular level, it requires a continuous adjustment of the hand translation and orientation to transfer exactly the desired amount of liquid into the target receptacle. Humans’ hand motion planning systems are remarkably robust in adapting to unseen objects, emulating movements observed from others, and devising paths from visual cues alone. Robotic agents and AI systems alike could benefit immensely from a similar ability to synthesize 3D hand trajectories from an image depicting a hand-object interaction scenario, be it to anticipate human behavior, generate realistic animations, or interact with the physical world. Following this realization, we wish to investigate the generation of high-quality hand trajectories from visual representations of objects.

✉ Correspondence to agavryushin@ethz.ch

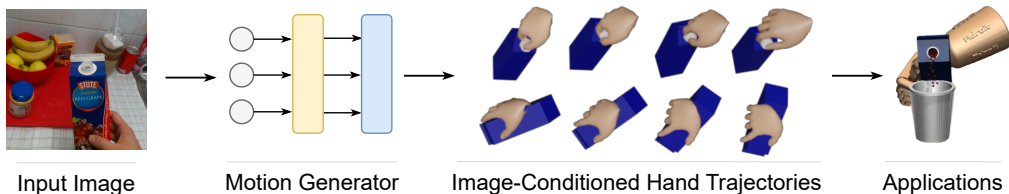


Figure 1: **Task description.** Given an input image showing an object, either being interacted with by a hand or pictured by itself, we propose the novel SIGHT task, requiring the generation of task-adequate, diverse, and realistic hand sequences mapping out possible trajectories of the hand when interacting with the object as shown. The task has applications in robotics, character animation, and human intent prediction, among others.

In this paper, we propose the new task of *Single-Image Conditioned Generation of Hand Trajectories* (SIGHT). Given a single first-person image showing a hand interacting with an object, our goal is to generate plausible and diverse 3D hand trajectories that meaningfully complete the action initiated in the image. Additionally, we explore the generation of appropriate interaction trajectories from standalone images of previously unseen objects without a hand manipulating the object.

Previous studies on hand-object interactions concentrate on detecting and segmenting (Darkhalil et al. (2022); Zhang et al. (2022a)) pairs of hands and objects interacting within images, or aim to reconstruct the 3D models of objects and the hands interacting with them from images (Hasson et al. (2019); Ye et al. (2022)) or videos (Fan et al. (2024); Ye et al. (2023a)), but do not generate novel trajectories. Furthermore, the field of human motion generation has hitherto focused on whole-body motion synthesis (Guo et al. (2022; 2020b); Tevet et al. (2022)), with little attention paid to synthesizing realistic, task-appropriate and interactive hand motions. The conditional information in previous whole-body motion synthesis work is restricted to either action labels or textual descriptions of motions, inconveniently requiring manual text annotations or action descriptions alongside the motion data. In contrast, our main focus is on generating dynamic 3D hand trajectories from a single static image. We utilize an underexplored and more easily affordable form of conditioning motion generation models to generate motions for an important yet neglected facet of human motion. Our aim is to reduce the amount of conditional information provided, restricting it solely to the static hand-object interaction or standalone object portrayed in the input image. Diverging from prior hand-object interaction tasks, the new proposed task, SIGHT, has a more generic but challenging setup, considering the multitude of possible hand-object interactions and the minimal guidance information provided.

SIGHT comes with several challenges. When generating trajectories from first-person hand-object interaction images, the initial step in addressing this task is to detect the interacting hand and object, as images captured from a real-world first-person perspective often exhibit significant clutter in the background. Moreover, generating future hand trajectories from images capturing static moments of interaction involves disambiguating the intended action, with objects often having multiple possible uses corresponding to different hand trajectories. The points of contact between the hand and the object play a key role in differentiating between similar actions, although hand and object often occlude each other in the images. Further, synthesizing sequences of hand trajectories necessitates the generation of smooth, natural and anatomically plausible motions that lead to the successful completion of the initiated actions for contacted objects. Finally, an interaction trajectory generation system integrated into the real world must operate robustly even when presented with previously unseen objects, complicating the inference of object-appropriate trajectories.

We present the SIGHT-Fusion method to address these challenges. Our key insight is in the meaningful identification of the contacted object in presence of distracting information in the input image’s background so as to maximally disambiguate the conditioning of the motion generator. Further, we find that egocentric videos of people interacting with diverse objects can serve as an effective source of training data for reasoning about interaction trajectories fitting previously unseen object instances. The effective use of visual hand-object interaction features enables our model to infer the underlying intentions and generate realistic hand trajectories for the intended interactions depicted in a single image. More specifically, SIGHT-Fusion is a conditional motion generation diffusion model that learns to generate realistic and diverse 3D hand trajectories. The extracted hand-object interaction features are used as the conditional input. Through training, SIGHT-Fusion learns the

distribution of possible hand movements given a static interaction moment and acquires the ability to distinguish between potential plausible motion sequences by leveraging fine-grained details contained in the contact regions. Using a general-purpose vision foundation models for the extraction of object features, SIGHT-Fusion effectively generalizes to object instances not seen during training.

We set up comprehensive baselines and metrics utilizing the FPHAB (Garcia-Hernando et al. (2018)) and HOI4D (Liu et al. (2022)) datasets for the newly proposed SIGHT task. Extensive experiments demonstrate that SIGHT-Fusion is able to generate more natural and diverse hand trajectories than baselines. We also observe promising potentials for our learned system to generalize to unseen object instances. We further introduce a task-oriented metric to execute the generated hand trajectories in physical simulation and evaluate if they could lead to successful task execution. Results show that our method is able to produce trajectories that can accomplish downstream tasks successfully. Lastly, we empirically validate system designs including the usefulness of various feature types in improving the quality of our result.

In summary, the contributions in this paper are as follows: 1) We introduce a novel task of generating 3D hand trajectories given a single image of an object, in the two settings of either being depicted by itself or being interacted with by a human hand. 2) We set up comprehensive benchmarks for the new task, including various baselines and metrics. We further propose a task success rate metric for evaluation using physical simulation. 3) We develop SIGHT-Fusion to tackle the proposed problem with a novel pipeline to extract hand-object interaction features from the single image input and a conditional diffusion-based hand trajectory generative model. 4) Experiments show superior performance compared with baselines and ablated versions of our system.

2 RELATED WORK

The field of learning hand-object interactions, particularly in first-person videos, has seen growing interest. We briefly discuss existing methods for hand-object interaction segmentation, 3D hand reconstruction, and motion generation.

Hand-Object interaction segmentation. Advancing the domain of interaction detection, Shan et al. (Shan et al. (2020)) introduce a method based on Faster-RCNN (Ren et al. (2015)) to detect hands and objects from RGB images, utilizing RoI features for predicting hand sides, bounding boxes, and contact states. EgoHOS (Zhang et al. (2022a)), adopting a similar framework, enhances the methodology by training on diverse first-person datasets and adding the capability to predict the contact boundary between hands and objects. In a different approach, COHESIV (Shan et al. (2021)) generates detailed pixel-wise features, enabling the segmentation of images into classes of people, objects, and backgrounds. This segmentation process is augmented by a user-defined query point on the visible hand, utilizing optical flow and regressed hand poses to improve accuracy.

Whole-body motion generation. Recent work in motion generation has relied heavily on Variational Auto Encoders (VAE) and Diffusion models. Studies have explored conditional generation using text (Karunratanakul et al. (2023); Kim et al. (2023); Tevet et al. (2023); Zhang et al. (2022b)), audio (Yi et al. (2023)), both (Dabral et al. (2023); Zhou & Wang (2022)) and categorical actions (Zhao et al. (2023)). Tevet et al. (Tevet et al. (2023)) expand upon previous work (Kim et al. (2023); Zhang et al. (2022b)) by introducing a classifier-free diffusion model MDM for text-driven full-body human motion generation. Other works such as (Diomataris et al. (2024)) also generate full-body human motions using c-VAEs. GMD (Karunratanakul et al. (2023)) further enhances it by adding spatial constraints. Most works such as (Petrovich et al. (2022b)) use VAE’s to generate diverse SMPL body shapes from texts, while others (Yi et al. (2023); Zhang et al. (2023)) use a Vector Quantised VAE (VQ-VAE) to generate human poses from text and speech respectively. A hybrid approach combining VAEs and diffusion models by (Chen et al. (2023)) de-noise conditional latent vectors and decode them to produce human body poses.

Hand motion generation. A novel two-step method is introduced in Ye et al. (2023b) for synthesizing hand-object interaction images from a single RGB image of an object using diffusion models. This method, however, generates static snapshots rather than a continuous motion. Other works such as HMP (Duran et al. (2023)) try to generate 3d hand poses even if the hand is occluded. All of these approaches have the disadvantage that they generate snapshots rather than full motions which is what has been done for full body movements. Bao et al. (2023) tries to predict hand movement

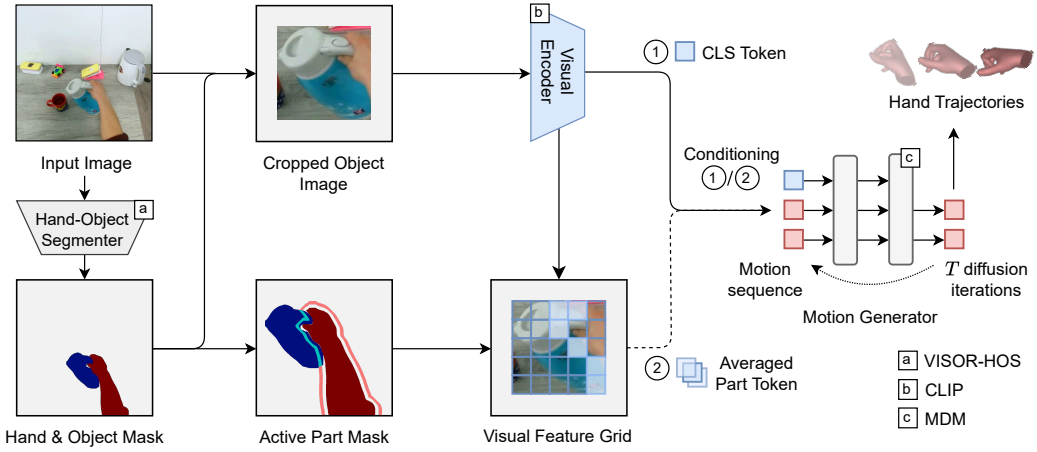


Figure 2: **Method description.** Given the input image, we first use a hand-object interaction detection system to locate the interacted object and hand, after which we extract object and part features from the image. The features are forwarded to a diffusion-based motion generator, which produces task-appropriate and realistic hand trajectories.

for a VR/AR setting however it only predicts the general motion and not the precise movement of individual joints. AI often has problems with generating accurate and precise hands, which is often used as a telltale sign to differentiate actual images from generated ones.

Motion in simulator. Manipulation tasks using hands inside a physical environment is a challenging as integrating forces such as gravity and current velocity of an object can render seemingly good trajectories bad. When considering the task of pouring juice into a glass moving the juice bottle with to much speed quickly leads to liquids spilling in all directions. Work in this area uses methods such as RL learning (Rajeswaran et al. (2018)) to generate 3D realistic motions. Some prior works explored using physical simulators to evaluate the stability of synthesized grasps (Yang et al. (2021); Wang et al. (2024)), considering only a static scenario. However, to the best of our knowledge, there have not been any efforts where the authors try to evaluate the physical realism of their generated trajectory with a physical simulator.

3 METHOD

In this section, we start by formulating the SIGHT task (Section 3.1). We then detail our feature extraction method (Section 3.2), which is used to obtain conditioning inputs for training and synthesizing hand trajectories with our motion generation model SIGHT-Fusion. Finally, we describe our model design for generating accurate, diverse, and realistic hand trajectories (Section 3.3). Our feature extraction method and model are visualized in Figure 2.

3.1 TASK DEFINITION

We consider two variations of our task: in our first setup, the input \mathcal{I} to the hand motion generator \mathcal{M} is a first-person image showing a hand enacting a certain action on an interacted object, such as *opening* or *pouring out* a bottle. In our second setup, \mathcal{I} consists of a close-up image showing an object without an interacting hand. For both cases, the expected output is a sequence of hand poses $\mathcal{H}_{1:f} = \mathcal{H}_1, \dots, \mathcal{H}_f$, where f is a predefined number of frames. Each \mathcal{H}_i corresponds to a representation of a 3D human hand for a single timestep. Our work represents the \mathcal{H}_i using SMPL-X (Pavlakos et al. (2019)) and reasons about the right hand, in concordance with the predominantly right-handed object interactions seen in most publically available video datasets.

3.2 EXTRACTING ACTION-INFORMATIVE FEATURES

Given an input image, the SIGHT task requires extracting highly informative visual features to guide the motion synthesis. When generating hand trajectories from images depicting hand-object inter-

action scenarios, correctly identifying the object of interest in the input frame presents a challenge due to background clutter and occlusion caused by the hand. The synthesis of a correct motion is even more difficult when generating trajectories from images of standalone objects not including manipulating hands, as no interaction cues are given.

Object features. We first use VISOR-HOS (Darkhalil et al. (2022)) to detect interacted objects \mathcal{O} in the input images \mathcal{I} , and then crop to the bounding box of \mathcal{O} before extracting visual features. See the Supp. Mat. for details about the training of VISOR-HOS. The visual object features are obtained using CLIP (Radford et al. (2021)) to leverage the generalizability of foundation model features, helping us reason about objects not seen during training.

Part features. Furthermore, we investigate providing the motion generator with additional conditioning information in the form of features local to the contact point between the hand and the object. We extract features from high-level CLIP 2D feature grids and use them as part features. Our hypothesis is that part features help to disambiguate different actions that are associated to different object parts. We begin by dilating the HOS hand mask and intersecting the dilated mask with the HOS object mask. The resulting mask is then cropped to the region of \mathcal{O} and resized to match the dimension of the 2D CLIP feature grid. An average feature vector is computed by taking the mean of all grid patches within the resized mask region. This vector is linearly projected to the input dimension of our Transformer (Vaswani et al. (2017))-based motion generator and prepended to the input motion sequence.

3.3 LEARNING TO GENERATE HAND TRAJECTORIES

Denoising diffusion models, originally proposed for image synthesis (Rombach et al. (2022); Saharia et al. (2022)), have been successfully adapted to whole-body human motion generation (Tevet et al. (2022); Karunratanakul et al. (2023); Yuan et al. (2023)). These models surpass traditional methods based on GANs (Barsoum et al. (2018); Guo et al. (2020b)) and VAEs (Petrovich et al. (2021; 2022a)) by delivering superior quality and diversity in generated motions. Given the shared requirement of reasoning about temporal sequences of joints, we adapt the Human Motion Diffusion Model (MDM) (Tevet et al. (2022)) for the SIGHT task of 3D hand trajectory generation. Originally, MDM synthesizes whole-body human motions from text inputs or learned embeddings encoding action labels. The motion synthesis process for a sequence of N frames, represented by J joints with R features each, starts with a randomly sampled latent code $x_T \sim \mathcal{N}(0, I)$ where $x_i \in \mathcal{R}^{N \times J \times R} \forall i \in \{1, \dots, N\}$, and uses a transformer \mathcal{G} to iteratively diffuse the final motion x_0 in T steps.

We employ a Transformer encoder model to iteratively diffuse the synthesized motion, starting from Gaussian noise. During each diffusion iteration, the Transformer receives as input the conditioning information contained in the initial tokens, followed by tokens representing the motion sequence from the previous diffusion step, or Gaussian noise for the initial step (see Figure 2). Our work does not consider the prediction of manipulation trajectories for multiple objects being manipulated by the actor simultaneously, as this is a highly specific setup with little publicly available data.

We repurpose MDM for hand trajectory generation by replacing the original whole-body kinematic tree with the representation of the right hand used by OpenPose (Cao et al. (2017)) and SMPL-X (Pavlakos et al. (2019)), yielding $J = 17$ joints. We also replace the original textual encoder used for conditioning inputs with CLIP’s visual encoder. We maintain the 6-dimensional pose representation used by MDM to encode motions, i.e. $\mathcal{R} = 6$, as suggested by (Zhou et al. (2019)).

To train our motion generator, we adapt the simple position and velocity losses from Tevet et al. (2022) while dropping the foot contact loss. Specifically, let c be the conditioning information, FK be a forward kinematics function reconstructing 3D hand joints from 6D pose representations, r and \hat{r} be the original and reconstructed 6D pose representations, and x_t^i be the full pose representation at diffusion step $t \in \{1, \dots, T\}$ for frame $i \in \{1, \dots, N\}$. During every diffusion step t , we concatenate the input conditioning information c with x_t to form the input of \mathcal{G} , which is trained to predict the final motion sequence from this condition-augmented intermediate representation. Our optimized loss term \mathcal{L} hence consists of:

$$\mathcal{L} = \mathcal{L}_{simple} + \lambda_{pos} \mathcal{L}_{pos} + \lambda_{velocity} \mathcal{L}_{velocity}, \quad (1)$$

where

$$\mathcal{L}_{simple} = \mathbb{E}_{x_0 \sim q(x_0|c), t \sim [1, T]} [\|x_0 - \mathcal{G}(x_t, t, c)\|_2^2],$$

$$\mathcal{L}_{pos} = \|FK(r) - FK(\hat{r})\|_2^2,$$

$$\mathcal{L}_{velocity} = \frac{1}{N-1} \sum_{i=1}^{N-1} \|(x_0^{i+1} - x_0^i) - (\hat{x}_0^{i+1} - \hat{x}_0^i)\|_2^2.$$

4 EXPERIMENTS

We demonstrate the effectiveness and generality of our proposed SIGHT-Fusion on a diverse set of in-the-wild egocentric videos. We first introduce the experimental setup in Section 4.1. Next, we show the quantitative and qualitative evaluation results of the generated hand trajectories in Section 4.2, and highlight the model’s ability to generalize to unseen objects in Section 4.5. Lastly, we evaluate the generated hand trajectories in a physics simulator, demonstrating the physical realism of the generated motion sequences (Section 4.6).

4.1 DATASETS

To establish a comprehensive evaluation for our newly introduced task, we adapt two first-person video datasets for our benchmark. We also introduce new dataset splits to test adaptability to unseen scene backgrounds and new object instances.

FPHAB (Garcia-Hernando et al. (2018)) The FPHAB dataset contains first-person videos capturing 45 activities (defined as action-object pairs, e.g. *stir cup*), involving 26 objects. Each activity is recorded multiple times by six different subjects, all using their right hands. Motion-captured hand poses are provided together with the video data. Following the human motion generation literature, we first merge all actions of the same verb, disregarding the corresponding objects (to be elaborated in Sec. 4.2). We further eliminate videos without any object manipulation, such as those where a simple handshake is performed. We note that most of the frames in FPHAB contain hand-object interactions and pure object frames without occlusions are rare to find.

Preprocessing. Notably, the hands of all subjects in FPHAB exhibit significant occlusion due to motion capture markers, which leads to a performance deterioration of the off-the-shelf hand-object interaction detector used in our pipeline (Darkhalil et al. (2022)). To address this issue, we inpaint away these markers using a video inpainting method (Li et al. (2022)) prior to processing the dataset. Please refer to Supp. Mat. for detailed evaluation and visualizations.

Data split. We use the *cross-subject split* proposed in the original work, with subjects 1, 3 and 4 used for training, and the three others used for testing. As all actions, object categories and object instances appear in both the training and test sets, this original FPHAB split poses a simple test verifying the generalizability of models to novel views of object instances and actions already seen in the training set. However, the high number of objects and the association of multiple actions with the same object category make inferring the correct action to synthesize appropriate hand trajectories particularly challenging for this dataset.

HOI4D (Liu et al. (2022)) The HOI4D dataset consists of first-person videos of hands interacting with everyday objects from 16 categories. The number of object instances varies within each category, ranging from 31 to 47, and the action tasks associated with these objects vary between 2 to 6 per category. Altogether, the dataset defines 31 action tasks. As many tasks are highly similar to each other or only involve a displacement of the object, we merge/ rename certain tasks and drop others to extract 13 *actions* from the original 31 tasks. Details of this grouping are provided in the Supp. Mat. As no public data split is available for HOI4D, we define our own splits with the aim of testing several dimensions of the generalizability for methods addressing the SIGHT task.

Instance split. For each object category and each action, there exist videos of at least 2 different object instances in HOI4D. This lends itself well to grouping the videos corresponding to different object instances of the same category and showing the same action being enacted. We then split

each group into one subgroup with instances to use only for the training set, and another subgroup with instances to use only for the test set. Our proposed *instance split* thus allows a meaningful evaluation of cross-instance action knowledge transfer. Simultaneously, more advanced reasoning is required for successful cross-instance transfer, as object instances in the test set may look different from those seen during training. Unlike in FPHAB, the videos in HOI4D do not start with the manipulated object already in hand. We thus construct the test frames for the instance split by cropping the first video frame to the yet ungrasped object of interest. Altogether, the instance split allows us to evaluate the setting of generating 3D hand trajectories for an unseen object, without interaction cues provided by the presence of a hand in the image. A detailed description of the proposed instance split is provided in the Supp. Mat.

Location split. We further wish to investigate generalizability for hand-object interaction scenes explicitly featuring hands in view. Since the HOI4D videos feature objects recorded at distinctive locations associated with specific actions, the background becomes more visible in the input image when expanding to a larger region to include the hand into the input image. We hence design the *location* split by dividing the HOI4D videos into training and test sets according to their recording location, i.e. the environment. Doing so reduces the possibility of data leakage about the action to synthesize through the image’s background. The location split hence provides an evaluation for the scenario of encountering both seen and novel objects in environments that are unseen during training.

In-contact frame selection. When constructing the test sets of our datasets in scenarios where the object and hand are in contact, we use VISOR (Darkhalil et al. (2022)) to detect the frame where the actor’s hand first contacts any object in each video. We then manually verify that the actor is indeed contacting the *desired* object. If necessary, we select a later frame that shows actual contact with the desired object. This manual adaptation is needed for only a few videos and is done to ensure the reliability of the test data used for evaluating methods.

4.2 EVALUATION OF GENERATED HAND TRAJECTORIES

Evaluation metrics. Following the combination of metrics that are commonly used in the human motion generation literature (Guo et al. (2020b); Tevet et al. (2022)), we measure a method’s success on our task based on the *accuracy*, *diversity*, and *fidelity to ground-truth* of its generated trajectories.

- **Accuracy (ACC):** Given that each generated hand trajectory is supposed to depict a specific action, we use the accuracy of an action classifier working on hand trajectories to measure the accuracy of the trajectories produced by a motion generation method \mathcal{M} . This formulation encourages the development of methods adept at matching their output trajectories to the hand-object interaction in the image given visual information alone, with no explicit knowledge of the desired output action.
- **Diversity (DIV):** The diversity of \mathcal{M} ’s outputs is calculated through the Fréchet Inception distances (FIDs) (Heusel et al. (2017)) between action classifier features extracted from generated and ground-truth motion groups. The diversity of the generated trajectories corresponds to the FID of one half of a trajectory group to the other half. It is desirable in moderation: too little diversity corresponds to a method simply (re-)producing a few learned trajectories, while too much results in the hand trajectories becoming erratic. Hence, a diversity score close to that of the GT trajectories is desirable.
- **Fidelity (FID):** The fidelity of hand trajectories generated by \mathcal{M} is calculated through the Fréchet Inception Distance (FID), similar to the diversity metric: lower FIDs between generated and ground-truth sequences translate to a motion generation method producing trajectories more similar in distribution to real reference trajectories.

Implementation details. For each run, consistent with the human motion generation literature (Guo et al. (2022; 2020a); Tevet et al. (2022)), we select the checkpoint achieving the lowest FID metric on the respective test set, so as to produce the trajectories most similar to the test set trajectories. Hyperparameters are provided in Supp. Mat.

Baselines. We compare our method against several strong baselines. As the proposed SIGHT task is novel and no existing approach is suitable for solving the task, we adapt state-of-the-art baselines from the whole-body motion generation literature. We evaluate both image-conditioned and text-



Figure 3: **Examples of generated trajectories.** We visualize hand trajectories generated by our \mathcal{P} model when conditioned on the given input images. We further visualize the inferred object regions (blue), as well as part regions (cyan) from which part features are calculated.

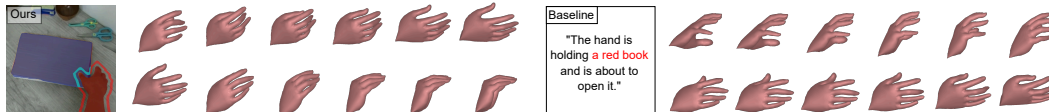


Figure 4: **Comparison with text-based baseline.** We visualize the input image, the inferred object (blue) and part (cyan) regions, the corresponding trajectory generated by our \mathcal{P} model in the upper row, as well as the VLM prompt output and the corresponding trajectory generated by the text-conditioned model MDM-T in the lower row. Contrary to the baseline, our method directly leverages visual features and produces an adequate trajectory by avoiding image-to-text translation errors from the VLM (see Sec. 4.2).

conditioned setups. The image conditioning features are produced as described in Sec. 3.2. The text conditioning is obtained by prompting LLaVa (Liu et al. (2023)), a state-of-the-art visual question answering model, with the question “*What is the hand in the image doing?*” given the input image cropped to the region of the manipulating hand and object. This text extraction helps mimic setups where we do not have access to ground-truth action annotations, as otherwise the synthesis task becomes trivial.

We evaluate against the following baselines in Table 1:

- **T2M-T** (Guo et al. (2022)): Similar to the original work, we first train a motion autoencoder to work with motion snippets. Next, we train a text encoder along with the decoder part of the motion autoencoder. We then integrate these components into a triplet variational autoencoder network to synthesize motions. As the original method is heavily adapted to textual conditioning, we only perform a text-based evaluation.
- **MDM-T** (Tevet et al. (2022)): MDM (Motion Diffusion Model) uses a Transformer embedded into a denoising process that gradually refines random noise into motions based on conditioning information, as described in Sec. 3.3. For MDM-T, we consider the original, text-based framework.
- **MDM-I** (Tevet et al. (2022)): This setup also uses MDM, but conditions on image features extracted from the *entire* image, without cropping to any object.

4.3 COMPARISON WITH STATE-OF-THE-ART

The evaluation results in Table 1 validate our hypothesis that conditioning on the interacted object leads to more appropriate trajectories, as evidenced by the increase in accuracy when visual features are used as input. The VLM-based image-to-text translation process is noisy and results in an inferior accuracy of the text-based methods, as also illustrated in the example comparison between T2M-T and our method in Fig. 4. This highlights the usefulness of visual input features for motion synthesis.

Compared to the evaluated baselines, our method is able to achieve superior performance in both accuracy and FID scores on the FPHAB dataset, as well as accuracy on the HOI4D location split.

Method	FPHAB (subject)			HOI4D (location)		
	ACC \uparrow	DIV \rightarrow	FID \downarrow	ACC \uparrow	DIV \rightarrow	FID \downarrow
Real	1.000	6.300	0.000	1.000	5.393	0.000
T2M-T, Guo et al. (2022)	0.124 \pm 0.011	6.258 \pm 0.070	0.809 \pm 0.078	0.730 \pm 0.022	5.348 \pm 0.179	1.851 \pm 0.360
MDM-T, Tevet et al. (2022)	0.284 \pm 0.016	6.545 \pm 0.087	0.818 \pm 0.058	0.771 \pm 0.025	5.680 \pm 0.280	1.050 \pm 0.015
MDM-I, Tevet et al. (2022)	0.358 \pm 0.008	6.417 \pm 0.076	0.826 \pm 0.028	<u>0.855</u> \pm 0.018	5.577 \pm 0.197	1.138 \pm 0.018
Ours, obj.	<u>0.413</u> \pm 0.009	6.546 \pm 0.091	0.764 \pm 0.001	0.854 \pm 0.011	<u>5.454</u> \pm 0.151	1.396 \pm 0.079
Ours, part	0.417 \pm 0.017	6.494 \pm 0.086	<u>0.805</u> \pm 0.054	0.885 \pm 0.011	5.518 \pm 0.162	1.436 \pm 0.164

Table 1: **Comparison with the state-of-the-art methods.** We compare our model SIGHT-Fusion with two other SOTA baselines and evaluate the generated hand trajectories on both FPHAB and HOI4D datasets. Note that here we use the location split of the HOI4D dataset. \rightarrow indicates that values closer to “Real” are better. We observe that our method outperforms the baselines in both ACC and FID metrics on the FPHAB dataset and achieves competitive results on the HOI4D location split. The results show that image features lead to better-generated trajectories in terms of ACC, and the use of part features yields better outcomes compared to object features. The best performance is highlighted in **bold**, while the second-best performance is underlined.

Experiment	Cond.	FPHAB (subject)		
		ACC \uparrow	DIV \rightarrow	FID \downarrow
Multi-action	\mathcal{O} -conditioned	0.359 \pm 0.016	6.226 \pm 0.147 \rightarrow 6.181	2.938 \pm 0.149
	\mathcal{P} -conditioned	0.450 \pm 0.022	6.064 \pm 0.114 \rightarrow 6.181	3.386 \pm 0.226
Single-action	\mathcal{O} -conditioned	0.486 \pm 0.015	6.409 \pm 0.110 \rightarrow 6.268	2.080 \pm 0.156
	\mathcal{P} -conditioned	0.504 \pm 0.025	6.376 \pm 0.073 \rightarrow 6.268	2.021 \pm 0.195
All actions	\mathcal{O} -conditioned	0.413 \pm 0.009	6.546 \pm 0.091 \rightarrow 6.300	0.764 \pm 0.001
	\mathcal{P} -conditioned	0.417 \pm 0.017	6.494 \pm 0.086 \rightarrow 6.300	0.805 \pm 0.054

Table 2: **Disambiguation by part features.** We single out 3 objects with multiple associated actions (juice bottle, milk bottle, salt), and evaluate the performance of our \mathcal{P} (part) and \mathcal{O} (object) models on these multi-action objects against the rest of the objects. The results show a clear increase in accuracy when using part features, particularly for multi-action objects. This indicates that actions are strongly related to object parts and part features help disambiguate the appropriate action.

We further achieve competitive results for the diversity on the HOI4D location split. Compared to object features, part features lead to better accuracy on both datasets. Examples of trajectories generated by our models are visualized in Figure 3. We encourage our readers to check the various video examples of generated hand trajectories included in the Supp. Mat.

4.4 DISAMBIGUATION OF ACTION BY PART FEATURES

To evaluate whether and how part features can help to disambiguate different actions, we conduct an experiment considering objects from the FPHAB dataset with multiple possible actions. These objects include *juice bottle*, *milk bottle* and *liquid soap*, and all of them are presented with the actions *open*, *close*, and *pour* in the dataset. Table 2 shows an increased accuracy (ACC) when using part features as conditioning information to the motion generator. This holds true for both the multi-action as well as the single-action objects, yet the benefit is particularly strong in the multi-action group. This confirms our intuition that features from the object part help disambiguate the type of action to synthesize for multi-action objects. Note that we consider the DIV and FID metrics less relevant here due to the purpose of the experiment, yet report them for completeness.

4.5 GENERALIZABILITY TO UNSEEN OBJECTS

To test how well our model generalizes across different object instances, we evaluate on the HOI4D instance split and compare our object-conditioned model with the MDM-I baseline. Results in Table 4.4 show that our method outperforms the baseline in terms of all metrics. By using object-centered visual features, we are able to generalize better to unseen object instances.

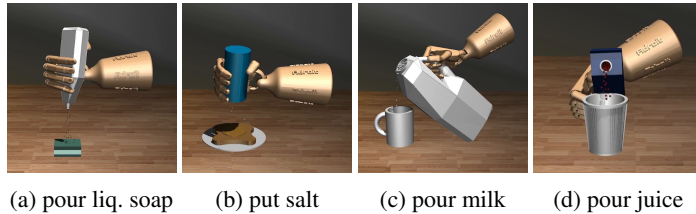
Cond.	HOI4D (instance)		
	ACC \uparrow	DIV \rightarrow	FID \downarrow
Real	1.000	5.814	0.000
MDM-I	0.734 \pm 0.011	5.547 \pm 0.156	1.380 \pm 0.081
Ours, obj.	0.909 \pm 0.006	5.780 \pm 0.120	0.624 \pm 0.050

Table 3: **Generalizability to unseen objects.** We evaluate generalization ability to unseen object instances on the HOI4D instance split and compare our model with the MDM baseline conditioned on image input. Our method outperforms the compared baseline on all metrics.

4.6 EVALUATION OF PHYSICAL PLAUSIBILITY IN SIMULATOR

As an additional evaluation of the physical realism and downstream usefulness of our generated trajectories, we design environments simulating the actions found in FPHAB using the MuJoCo simulator, introduced in Todorov et al. (2012).

Setup. We condition our \mathcal{P} model on images from the FPHAB test set, then retarget the generated human hand trajectories to a robotic hand according to Qin et al. (2021) to simulate corresponding object interactions and evaluate their success rates when executing the intended action. Specifically, we consider a total of four action-object combinations, referred to as *tasks*: *pour liquid soap*, *put salt*, *pour milk*, and *pour juice*. All evaluations of the generated trajectories start with the hand already grasping the object. The manipulated objects are initialized with several hundred particles inside. See the Supp. Mat. for details regarding the grasp initialization and trajectory retargeting. Visualizations of our environments are provided in Figure 5. Readers are further encouraged to consult the Supp. Mat. for videos of retargeted trajectories being enacted in the simulator.



(a) pour liq. soap (b) put salt (c) pour milk (d) pour juice

Figure 5: **Evaluating generated trajectories in a simulator.** We follow Qin et al. (2021) to retarget hand trajectories generated by our method to the robotic Adroit hand in the MuJoCo simulator. Afterwards, we evaluate the success rate of these trajectories in environments simulating the respective actions and objects. Our example environments are visualized here for the *pour liquid soap*, *put salt*, *pour milk*, and *pour juice* tasks.

Hit rate. For the *pour juice* and *pour milk* tasks, we simulate 280 resp. 480 spherical particles inside the opened juice/milk, and count how many particles landed inside a nearby cup out of all particles that left the container while executing the retargeted trajectory. We call this metric the *hit rate*. These two tasks require the hand to rotate the juice/milk in a controlled manner, as otherwise, the particles will immediately spill onto the floor. The receptacle (cup) slowly moves below the opening of the container (milk/juice) to catch falling particles, just as a second hand would move it during a pouring action. The *pour soap* and *put salt* tasks are similar in that a sponge resp. loaf of toast is following the container to catch emerging particles (200 for both tasks initially) whenever the salt resp. soap is shaken. Here, we again calculate the ratio of how many particles hit the receptacle out of all particles that left the container.

Object	Juice	Milk	Salt	Soap
% hit, GT	78.1	64.1	48.0	64.7
% hit, MDM-I	61.6	58.6	54.1	60.5
% hit, MDM-T	52.2	56.3	62.8	55.1
% hit, ours	84.4	65.6	54.6	60.1

Table 4: **Hit rates of generated trajectories.** We retarget the trajectories to a robotic hand and attempt to execute the action in MuJoCo. The favorable hit rates validate the physical realism of our generated trajectories and of our model’s inference capabilities given respective features.

due to the former being more suitable for the execution of the task if the objects were filled with liquid. When designing the objects in the simulator, we did not optimize for our method’s hit rate, and instead tried to imitate the shape of the original object from the FPHAB dataset as closely as possible.

5 CONCLUSION

In this work, we introduce the novel task of generating natural and diverse hand trajectories conditioned on single image inputs for hand-object interaction. Our work delves into the development of methodologies for this challenging problem, presenting not only straightforward baselines, but also examining advanced approaches by proposing the novel method SIGHT-Fusion. Various hand-object interaction features are extracted from the single image input, and a diffusion-based conditional hand trajectory generative model is trained without the need for supervision by action labels. We set up comprehensive baselines and metrics on the FPHAB and HOI4D datasets, and also propose novel physical simulation environments for additional evaluation. Experiments show our superior performance over baseline methods and promising results in generalizing to unseen objects. Ablation studies further assess and validate the effectiveness of our usage of part features as conditional information during the motion synthesis. We hope that our work will invite greater interest in the SIGHT task, and that our general-purpose pipeline will be of use in related problems such as action anticipation and hand trajectory reconstruction.

REFERENCES

Wentao Bao, Lele Chen, Libing Zeng, Zhong Li, Yi Xu, Junsong Yuan, and Yu Kong. Uncertainty-aware State Space Transformer for Egocentric 3D Hand Trajectory Forecasting, 2023.

Emad Barsoum, John Kender, and Zicheng Liu. HP-GAN: Probabilistic 3D Human Motion Prediction via GAN. In *Proceedings of the IEEE conference on computer vision and pattern recognition workshops*, pp. 1418–1427, 2018.

Zhe Cao, Tomas Simon, Shih-En Wei, and Yaser Sheikh. Realtime Multi-Person 2D Pose Estimation Using Part Affinity Fields. In *Proceedings of the IEEE Conference on Computer Vision and Pattern Recognition*, pp. 7291–7299, 2017.

Xin Chen, Biao Jiang, Wen Liu, Zilong Huang, Bin Fu, Tao Chen, Jingyi Yu, and Gang Yu. Executing your Commands via Motion Diffusion in Latent Space, 2023.

Rishabh Dabral, Muhammad Hamza Mughal, Vladislav Golyanik, and Christian Theobalt. MoFusion: A Framework for Denoising-Diffusion-based Motion Synthesis. In *Computer Vision and Pattern Recognition (CVPR)*, 2023.

Dima Damen, Hazel Doughty, Giovanni Maria Farinella, Antonino Furnari, Jian Ma, Evangelos Kazakos, Davide Moltisanti, Jonathan Munro, Toby Perrett, Will Price, and Michael Wray. Rescaling Egocentric Vision: Collection, Pipeline and Challenges for EPIC-KITCHENS-100. 130:33–55, 2022. URL <https://doi.org/10.1007/s11263-021-01531-2>.

Ahmad Darkhalil, Dandan Shan, Bin Zhu, Jian Ma, Amlan Kar, Richard Higgins, Sanja Fidler, David Fouhey, and Dima Damen. EPIC-KITCHENS VISOR Benchmark: VIdeo Segmentations and Object Relations. In *Proceedings of the Neural Information Processing Systems (NeurIPS) Track on Datasets and Benchmarks*, 2022.

Markos Diomataris, Nikos Athanasiou, Omid Taheri, Xi Wang, Otmar Hilliges, and Michael J. Black. WANDR: Intention-guided Human Motion Generation, 2024.

Edward R Dougherty. An Introduction to Morphological Image Processing. In *SPIE*. Optical Engineering Press, 1992.

Enes Duran, Muhammed Kocabas, Vasileios Choutas, Zicong Fan, and Michael J. Black. HMP: Hand Motion Priors for Pose and Shape Estimation from Video, 2023.

Zicong Fan, Maria Parelli, Maria Eleni Kadoglou, Muhammed Kocabas, Xu Chen, Michael J Black, and Otmar Hilliges. HOLD: Category-agnostic 3D Reconstruction of Interacting Hands and Objects from Video. 2024.

Guillermo Garcia-Hernando, Shanxin Yuan, Seungryul Baek, and Tae-Kyun Kim. First-Person Hand Action Benchmark With RGB-D Videos and 3D Hand Pose Annotations. In *Proceedings of the IEEE Conference on Computer Vision and Pattern Recognition*, pp. 409–419, 2018.

Chuan Guo, Xinxin Zuo, Sen Wang, Shihao Zou, Qingyao Sun, Annan Deng, Minglun Gong, and Li Cheng. Action2motion: Conditioned Generation of 3d Human Motions. In *Proceedings of the 28th ACM International Conference on Multimedia*, pp. 2021–2029, 2020a.

Chuan Guo, Xinxin Zuo, Sen Wang, Shihao Zou, Qingyao Sun, Annan Deng, Minglun Gong, and Li Cheng. Action2motion: Conditioned Generation of 3D Human Motions. In *Proceedings of the 28th ACM International Conference on Multimedia*, pp. 2021–2029, 2020b.

Chuan Guo, Shihao Zou, Xinxin Zuo, Sen Wang, Wei Ji, Xingyu Li, and Li Cheng. Generating Diverse and Natural 3D Human Motions From Text. In *Proceedings of the IEEE/CVF Conference on Computer Vision and Pattern Recognition (CVPR)*, pp. 5152–5161, June 2022.

Yana Hasson, Gul Varol, Dimitrios Tzionas, Igor Kalevatykh, Michael J Black, Ivan Laptev, and Cordelia Schmid. Learning Joint Reconstruction of Hands and Manipulated Objects. In *Proceedings of the IEEE/CVF Conference on Computer Vision and Pattern Recognition*, pp. 11807–11816, 2019.

Martin Heusel, Hubert Ramsauer, Thomas Unterthiner, Bernhard Nessler, and Sepp Hochreiter. GANs Trained by a Two Time-Scale Update Rule Converge to a Local Nash Equilibrium. *Advances in Neural Information Processing Systems*, 30, 2017.

Korrawe Karunratanakul, Konpat Preechakul, Supasorn Suwajanakorn, and Siyu Tang. GMD: Controllable Human Motion Synthesis via Guided Diffusion Models. In *CVPR*, 2023.

Jihoon Kim, Jiseob Kim, and Sungjoon Choi. FLAME: Free-form Language-based Motion Synthesis & Editing, 2023.

Zhen Li, Cheng-Ze Lu, Jianhua Qin, Chun-Le Guo, and Ming-Ming Cheng. Towards an End-To-End Framework for Flow-Guided Video Inpainting. In *Proceedings of the IEEE/CVF Conference on Computer Vision and Pattern Recognition*, pp. 17562–17571, 2022.

Haotian Liu, Chunyuan Li, Qingyang Wu, and Yong Jae Lee. Visual Instruction Tuning. In *NeurIPS*, 2023.

Yunze Liu, Yun Liu, Che Jiang, Kangbo Lyu, Weikang Wan, Hao Shen, Boqiang Liang, Zhoujie Fu, He Wang, and Li Yi. HOI4D: A 4D egocentric dataset for category-level human-object interaction. In *Proceedings of the IEEE/CVF Conference on Computer Vision and Pattern Recognition*, pp. 21013–21022, 2022.

Georgios Pavlakos, Vasileios Choutas, Nima Ghorbani, Timo Bolkart, Ahmed AA Osman, Dimitrios Tzionas, and Michael J Black. Expressive Body Capture: 3D Hands, Face, and Body From a Single Image. In *Proceedings of the IEEE/CVF Conference on Computer Vision and Pattern Recognition*, pp. 10975–10985, 2019.

Mathis Petrovich, Michael J Black, and Güл Varol. Action-conditioned 3d human motion synthesis with transformer vae. In *Proceedings of the IEEE/CVF International Conference on Computer Vision*, pp. 10985–10995, 2021.

Mathis Petrovich, Michael J Black, and Güл Varol. TEMOS: Generating Diverse Human Motions from Textual Descriptions. In *European Conference on Computer Vision*, pp. 480–497. Springer, 2022a.

Mathis Petrovich, Michael J. Black, and Güл Varol. TEMOS: Generating diverse human motions from textual descriptions, 2022b.

Qin, Yuzhe, Yueh-Hua Wu, Shaowei Liu, Hanwen Jiang, Ruihan Yang, Yang Fu, and Xiaolong Wang. DexMV: Imitation Learning for Dexterous Manipulation From Human Videos, 2021.

Alec Radford, Jong Wook Kim, Chris Hallacy, Aditya Ramesh, Gabriel Goh, Sandhini Agarwal, Girish Sastry, Amanda Askell, Pamela Mishkin, Jack Clark, et al. Learning Transferable Visual Models From Natural Language Supervision. In *International Conference on Machine Learning*, pp. 8748–8763. PMLR, 2021.

Aravind Rajeswaran, Vikash Kumar, Abhishek Gupta, Giulia Vezzani, John Schulman, Emanuel Todorov, and Sergey Levine. Learning Complex Dexterous Manipulation With Deep Reinforcement Learning and Demonstrations. 2017.

Aravind Rajeswaran, Vikash Kumar, Abhishek Gupta, Giulia Vezzani, John Schulman, Emanuel Todorov, and Sergey Levine. Learning Complex Dexterous Manipulation with Deep Reinforcement Learning and Demonstrations, 2018.

Shaoqing Ren, Kaiming He, Ross Girshick, and Jian Sun. Faster R-CNN: Towards Real-Time Object Detection With Region Proposal Networks. 28, 2015.

Robin Rombach, Andreas Blattmann, Dominik Lorenz, Patrick Esser, and Björn Ommer. High-Resolution Image Synthesis With Latent Diffusion Models. In *Proceedings of the IEEE/CVF Conference on Computer Vision and Pattern Recognition (CVPR)*, pp. 10684–10695, 2022.

Chitwan Saharia, William Chan, Saurabh Saxena, Lala Li, Jay Whang, Emily L Denton, Kamyar Ghasemipour, Raphael Gontijo Lopes, Burcu Karagol Ayan, Tim Salimans, et al. Photorealistic Text-To-Image Diffusion Models With Deep Language Understanding. *Advances in Neural Information Processing Systems*, 35:36479–36494, 2022.

Dandan Shan, Jiaqi Geng, Michelle Shu, and David F Fouhey. Understanding Human Hands in Contact at Internet Scale. In *Proceedings of the IEEE/CVF Conference on Computer Vision and Pattern Recognition*, pp. 9869–9878, 2020.

Dandan Shan, Richard Higgins, and David Fouhey. COHESIV: Contrastive Object and Hand Embedding Segmentation in Video. In M. Ranzato, A. Beygelzimer, Y. Dauphin, P.S. Liang, and J. Wortman Vaughan (eds.), *Advances in Neural Information Processing Systems*, volume 34, pp. 5898–5909. Curran Associates, Inc., 2021. URL https://proceedings.neurips.cc/paper_files/paper/2021/file/2e976ab88a42d723d9f2ee6027b707f5-Paper.pdf.

Kenneth Shaw, Shikhar Bahl, and Deepak Pathak. VideoDex: Learning Dexterity From Internet Videos, 2022.

Guy Tevet, Sigal Raab, Brian Gordon, Yonatan Shafir, Daniel Cohen-Or, and Amit H Bermano. Human Motion Diffusion Model. 2022.

Guy Tevet, Sigal Raab, Brian Gordon, Yoni Shafir, Daniel Cohen-or, and Amit Haim Bermano. Human Motion Diffusion Model. In *The Eleventh International Conference on Learning Representations*, 2023. URL <https://openreview.net/forum?id=SJ1kSyO2jwu>.

Emanuel Todorov, Tom Erez, and Yuval Tassa. MuJoCo: A Physics Engine for Model-Based Control. In *2012 IEEE/RSJ International Conference on Intelligent Robots and Systems*, pp. 5026–5033, 2012. doi: 10.1109/IROS.2012.6386109.

Ashish Vaswani, Noam Shazeer, Niki Parmar, Jakob Uszkoreit, Llion Jones, Aidan N Gomez, Łukasz Kaiser, and Illia Polosukhin. Attention Is All You Need. 30, 2017.

Rong Wang, Wei Mao, and Hongdong Li. DeepSimHO: Stable Pose Estimation for Hand-Object Interaction via Physics Simulation. *Advances in Neural Information Processing Systems*, 36, 2024.

Haotian Yan, Chuang Zhang, and Ming Wu. Lawin Transformer: Improving Semantic Segmentation Transformer With Multi-Scale Representations via Large Window Attention. 2022.

Lixin Yang, Xinyu Zhan, Kailin Li, Wenqiang Xu, Jiefeng Li, and Cewu Lu. CPF: Learning a Contact Potential Field to Model the Hand-Object Interaction. In *Proceedings of the IEEE/CVF International Conference on Computer Vision*, pp. 11097–11106, 2021.

Yufei Ye, Abhinav Gupta, and Shubham Tulsiani. What’s in Your Hands? 3D Reconstruction of Generic Objects in Hands. In *Proceedings of the IEEE/CVF Conference on Computer Vision and Pattern Recognition*, pp. 3895–3905, 2022.

Yufei Ye, Poorvi Hebbar, Abhinav Gupta, and Shubham Tulsiani. Diffusion-Guided Reconstruction of Everyday Hand-Object Interaction Clips. In *ICCV*, 2023a.

Yufei Ye, Xuetong Li, Abhinav Gupta, Shalini De Mello, Stan Birchfield, Jiaming Song, Shubham Tulsiani, and Sifei Liu. Affordance Diffusion: Synthesizing Hand-Object Interactions, 2023b.

Hongwei Yi, Hualin Liang, Yifei Liu, Qiong Cao, Yandong Wen, Timo Bolkart, Dacheng Tao, and Michael J. Black. Generating Holistic 3D Human Motion from Speech, 2023.

Ye Yuan, Jiaming Song, Umar Iqbal, Arash Vahdat, and Jan Kautz. Physdiff: Physics-Guided Human Motion Diffusion Model. In *Proceedings of the IEEE/CVF International Conference on Computer Vision*, pp. 16010–16021, 2023.

Jianrong Zhang, Yangsong Zhang, Xiaodong Cun, Shaoli Huang, Yong Zhang, Hongwei Zhao, Hongtao Lu, and Xi Shen. T2M-GPT: Generating Human Motion from Textual Descriptions with Discrete Representations, 2023.

Lingzhi Zhang, Shenghao Zhou, Simon Stent, and Jianbo Shi. Fine-Grained Egocentric Hand-Object Segmentation: Dataset, Model, and Applications. In *European Conference on Computer Vision*, pp. 127–145. Springer, 2022a.

Mingyuan Zhang, Zhongang Cai, Liang Pan, Fangzhou Hong, Xinying Guo, Lei Yang, and Ziwei Liu. Motiondiffuse: Text-driven human motion generation with diffusion model. *arXiv preprint arXiv:2208.15001*, 2022b.

Mengyi Zhao, Mengyuan Liu, Bin Ren, Shuling Dai, and Nicu Sebe. Modiff: Action-Conditioned 3D Motion Generation with Denoising Diffusion Probabilistic Models, 2023.

Yi Zhou, Connelly Barnes, Jingwan Lu, Jimei Yang, and Hao Li. On the Continuity of Rotation Representations in Neural Networks. In *Proceedings of the IEEE/CVF Conference on Computer Vision and Pattern Recognition*, pp. 5745–5753, 2019.

Zixiang Zhou and Baoyuan Wang. UDE: A Unified Driving Engine for Human Motion Generation, 2022.

A SUPPLEMENTARY MATERIAL



Figure 6: **VISOR-HOS performance on non-inpainted vs. inpainted FPHAB.** We visualize VISOR-HOS’ output on pairs of the non-inpainted RGB image (left) and the corresponding inpainted image (right).

A.1 GENERATION OF VISUALIZATIONS.

The hand-object trajectory visualizations in this work are generated by first performing an iterative optimization minimizing the distances between predefined hand mesh vertices and object contact points, then updating the rotation of the hand to follow the rotation of predefined finger joint pairs (e.g. the wrist-to-index rotation in case of “pour milk”).

A.2 INPAINTING FPHAB MOTION CAPTURE MARKERS.

The performance of the employed hand-object interaction detection model (Darkhalil et al. (2022)) suffers significantly from the motion capture (mocap) markers visible on the subjects’ hands in FPHAB. To counteract the problem, we train a Lawin (Yan et al. (2022)) model to segment the mocap markers in each frame after manually creating a small segmentation dataset, then use the E2FGVI (Li et al. (2022)) model to inpaint the mocap markers away after segmenting them on the entire dataset. Visualizations are provided in Figure 6.

A.3 HYPERPARAMETERS

MDM. Our MDM (Tevet et al. (2022))-based models are trained for 250K steps, using a batch size of 32 and a learning rate of 10^{-4} with the Adam optimizer. We set MDM’s T parameter to $T = 1000$ to perform 1000 diffusion steps per motion, and further use $\lambda_{pos} = \lambda_{vel} = 1, \lambda_{foot} = 0$ for MDM. When evaluating and generating motions, we set the number of frames to generate to $n_f = 200$ so as to cover the vast majority of the motion length distribution of both employed datasets. A guidance parameter of $s = 2.5$ and a latent embedding size of $d = 512$ is used.

Part feature extraction. We use the `scipy.ndimage.binary_dilation` function of the `scikit-learn` package to compute the dilated hand masks described in subsection 3.2. 7 dilation iterations are used to obtain the first mask, and 15 dilation iterations are used to obtain the second mask. The second mask hence fully includes and extends the first mask. A single dilation iteration can be thought of as approximately isotropically extending the mask obtained by the previous dilation operation. Please see Dougherty (1992) for the full description of a dilation iteration.

We use 2D CLIP feature grid patches falling into the second dilated hand mask, but not the first dilated hand mask, to compute the part feature vectors. At the same time, the used patches must also fall into the region of the object mask, which we do not dilate. The idea is to include rectangular patches close to the contact region (use of the dilated hand mask) and limited to the object (use of the object mask), but not showing the hand/fingers (subtraction of the undilated hand mask from the object mask).

Whenever part features are employed, they are used in combination with object features. This is accomplished by providing a separate part feature conditioning token together with the object feature conditioning token to the motion generator, which is always provided.

action	original task(s)	object categories	instances in training set	instances in test set
bind	bind the paper	stapler	27	11
clamp	clamp something	pliers	23	9
cut	cut something	scissors	28	12
enable/ disable	turn on and turn off	lamp	-	-
fill	fill with water by a kettle	mug	7	2
move	pick and place	bottle, bowl, bucket, kettle, knife, lamp, laptop, mug, pliers, scissors, stapler, toy car	18, -, 23, 28, 28, -, 25, 25, 28, 26, 28, -	5, -, 9, 12, 12, -, 9, 11, 11, 10, 12, -
	pick and place to original position	chair	-	-
	pick and place to new position	chair	-	-
	pick and place with ball	bowl	-	-
	pick and place with water	bottle, mug	16, 13	8, 3
open/close	open and close	trash can	-	-
	open and close the display	laptop	33	13
	open and close the door	storage furniture	-	-
	open and close the drawer	storage furniture	-	-
pour	pour all the water into a mug	bottle	24	9
	pour water into a mug	kettle	28	12
	pour water into another mug	mug	14	5
	pour water into another bucket	bucket	27	11
push	push toy car	toy car	-	-
retrieve	take it out of the drawer	bottle, bowl, knife, pliers, toy car	19, -, 12, 23, -	8, -, 4, 9, -
	take something out of it	safe	-	-
	take the ball out of the bowl	bowl	-	-
slice	cut apple	knife	26	10
store	put it in the drawer	bottle, bowl, knife, mug, pliers	10, -, 15, 19, 19	4, -, 6, 8, 7
	put the drink in the door	storage furniture	-	-
	put the drink in the drawer	storage furniture	-	-
	throw something in it	trash can	-	-
turn	turn and fold	lamp	-	-

Table 5: **Actions for the HOI4D instance split.** Our proposed action-centric *instance split* for the HOI4D dataset, assigning each instance to either the train or the test set for each object and action. In this work, we train and evaluate on the objects *bottle*, *bucket*, *kettle*, *knife*, *laptop*, *mug*, *pliers*, *scissors*, *stapler*, retaining a total of 10 from the 13 proposed actions.

A.4 HOI4D INSTANCE SPLIT

We list the *actions* derived from the original tasks proposed by HOI4D, as well as the corresponding instance counts per action and object category in the training and test set of our HOI4D instance set in Table 5.

A.5 DETAILS ON SIMULATION EXPERIMENTS

A.5.1 HAND TRAJECTORY RETARGETING

We use the Adroit hand model employed by Rajeswaran et al. (2017) to evaluate our trajectories in the simulator. This necessitates a conversion of the SMPL-X hand trajectory to a functionally equivalent trajectory where the Adroit hand is used. One of the commonly employed paradigms for this conversion is the vector-based approach introduced in Shaw et al. (2022). It proposes solving a quadratic optimization problem during each timestep to solve for the joint rotations of the robotic hand. The optimization aims to make the distances between the human fingertips observed during the manipulation match the distances between the agent’s fingertips, as well as align the palm-fingertip distances in the same manner. Temporal smoothing is further used to stabilize the resulting retargeted trajectory. Please consult Shaw et al. (2022) for further details.

A.5.2 HAND TRAJECTORIES TO ACTUATOR ACTIVATIONS

The MuJoCo simulator requires the simulation script to provide actuator activations during each environment step. This necessitates a conversion from the 6D hand joint representation our model employs to a representation of the motion in terms of actuator activations.

A.5.3 GRASP INITIALIZATION

As the synthesis of a grasp that holds the object in place and avoids hand-object penetration is highly challenging and outside the scope of our work, we initialize the hand trajectories evaluated in the simulator with manually defined grasps. After the initialization, we follow the trajectory synthesized by the respective model by applying the calculated joint actions, as described in subsubsection A.5.2. Additionally, we apply a strong bias on multiple mid-finger actuators, which causes the hand to squeeze the held object and thereby prevent the object from slipping out of the hand.

A.6 TRAINING OF VISOR-HOS

The VISOR-HOS (Darkhalil et al. (2022)) model that we use to identify interacted objects is trained on a subset of the egocentric EPIC-KITCHENS 100 (Damen et al. (2022)) dataset. The subset is a combination of a small number of frames with manually annotated interacted object masks, and a large number of frames with interacted object masks automatically interpolated using the sparse manually annotated masks. The class of the interacted objects is not predicted. In total, 14.5M masks are used during training and 3.2M are used during validation to train the segmentation model. Please refer to Darkhalil et al. (2022) for further details.

A.7 DATASET SIZES

After processing the videos, we obtain 3860 resp. 542 samples for the train resp. validation split of the FPHAB dataset. For the HOI4D dataset, we obtain 3954 resp. 169 samples for the instance split, and 5014 resp. 104 samples for the location split.

A.8 COMPUTE RESOURCES

For training all diffusion models, we used an RTX-4090. The training of one such model for 250.000 epochs takes approximately 36 hours. For evaluation using the MuJoCo simulator, we used an AMD EPYC 7742 CPU with 128 cores. Evaluating 50 trajectories in simulation takes circa 2 hours.